

## Original Research Article

# Electrochemical determination of $\text{Hg}^{2+}$ on a poly(Eriochrome blue black R) modified carbon paste electrode

### ABSTRACT

In this work a new, simple, fast, and efficient electrochemical approach for the determination of inorganic mercury ( $\text{Hg}^{2+}$ ) using the differential pulse anodic stripping voltammetry (DPASV) technique was presented. This is achieved by modifying the surface of a carbon paste electrode by electropolymerization of Eriochrome blue black R. First, the behavior of  $\text{Hg}^{2+}$  on the modified electrode is studied by cyclic voltammetry and electrochemical impedance spectroscopy, to evaluate performance and understand the phenomena that take place on its surface. DPASV is then used to optimize the sensor in  $\text{HClO}_4$  medium. After optimization, a linear calibration graph was obtained in the concentration range of  $1 \times 10^{-9}$  to  $9 \times 10^{-9} \text{ mol.L}^{-1}$  with correlation coefficient  $R^2 = 0.9975\%$ , the limit of detection (LOD) and the limit of quantification (LOQ) obtained are respectively  $3.23 \times 10^{-10} \text{ mol.L}^{-1}$  and  $1.07 \times 10^{-9} \text{ mol.L}^{-1}$ . The relative standard deviation (RSD) for 7 measurements is 3.07%, which proves that this sensor is reproducible. Finally, this method has been successfully applied in real samples of water and the results obtained are satisfactory because the recovery rates of  $\text{Hg}^{2+}$  vary from 99.2 to 100.1%.

*Keywords:* Carbon paste electrode, poly(Eriochrome blue black R), inorganic mercury(II), differential pulse anodic stripping voltammetry.

### 1. INTRODUCTION

Mercury (Hg) is one of the representative heavy metals, is ranked third on the list of toxicological dangerous substances by the United States Toxicology and Disease Registry [Error! Reference source not found.]. Hg is emitted into the environment from anthropogenic activities or natural sources [Error! Reference source not found.]. Anthropogenic actions such as inappropriate industrial waste management and illegal artisanal gold mining resulted in Hg contamination of ecosystems leading to the public health concern [Error! Reference source not found.] caused by chronic exposure through the intake of food and water [Error! Reference source not found.]. Species of Hg determine its environmental transport, bioavailability, and toxicity [Error! Reference source not found.]. The inorganic mercury ion ( $\text{Hg}^{2+}$ ) is the dominant form of mercury in water. Exposure to  $\text{Hg}^{2+}$  directly damages the human brain, nervous system, kidneys, and endocrine system [Error! Reference source not found.]. Inorganic mercury tends to accumulate in the kidneys, leading to renal failure [Error! Reference source not found.]. Similarly, exposure to inorganic mercury has been shown to disrupt the reproductive system and induces testicular immunosuppression and fibrosis via inhibition of the CD74 (antigen) signaling pathway in male mice [Error! Reference source not found.].

The global issue of Hg was confronted by the adoption of the Minamata Convention, in 2017 under the auspices of UNEP (United Nations Environmental Protection) to reduce human and ecosystem Hg exposure [Error! Reference source not found.]. For this reason, the acceptable limit of inorganic mercury  $\text{Hg}^{2+}$  in drinking water has been set by the World Health Organization (WHO) and the US Environmental Protection Agency (EPA) as  $30 \text{ nmol.L}^{-1}$  and  $10 \text{ nmol.L}^{-1}$ , respectively [Error! Reference source not found.]. Therefore, there is a great desire to design reliable methods that are sensitive, selective and efficient for the determination of  $\text{Hg}^{2+}$ , especially in water. Many analytical methods have been proposed, including HPLC-ICP-MS [Error! Reference source not found.], non-chromatography atomic spectroscopy [Error!

Reference source not found.], fluorescence sensing [Error! Reference source not found.], and surface-enhanced Raman scattering [Error! Reference source not found.]. Although these methods show excellent detection performance, most of them require expensive precision instruments, complex sample preparation processes, skilled operators and they cannot be conveniently used online or outdoors [Error! Reference source not found.]. To overcome these limitations, attention has turned to voltammetry, in particular differential pulse anodic stripping voltammetry (DPASV), due to its ability to achieve high sensitivity and selectivity. Additionally, it is user-friendly, allows rapid analysis, is relatively inexpensive and is highly suitable for in situ applications [Error! Reference source not found.]. Several materials have been used for the modification of the surface of the working electrode. Emerging polymers are generally believed to be signal enhancers in electroanalytical operations from characteristics such as higher conductivity, lighter weight, more flexibility, simplified procurement and greater numbers of active sites as well as stronger adherence to the surface of the electrodes [Error! Reference source not found.]. Several polymers have been investigated for the modification of the surface of the carbon paste electrode (CPE) by DPASV for the detection of  $\text{Hg}^{2+}$ . These include poly(2,2'-dithiodianiline) [Error! Reference source not found.], poly(Eriochrome black T) [Error! Reference source not found.], polyglycine [Error! Reference source not found.], Poly(3-hexylthiophene) [Error! Reference source not found.], poly(3,4-ethylenedioxythiophene) nanorods/graphene oxide [Error! Reference source not found.].

In this paper we report construction of a new chemically modified CPE for the determination of  $\text{Hg}^{2+}$  in aqueous medium. Eriochrome blue black R (Calcon) dye was used to form a film polymer in a basic medium to modify the surface of CPE by cyclic voltammetry. The optimization of the operating analytical parameters, such as polymer concentration, solution and concentration of the supporting electrolyte, potential and time to deposit the film, stirring of solution, and some differential pulse voltammetry parameters were studied. In addition, the calibration plot, limit of detection, limit of quantification and interfering ions are investigated to evaluate the metrological performances. Finally, the analytical analysis of real samples was tested using well water.

## 2. EXPERIMENTAL PART

### 2.1. Apparatus

Electrochemical experiments were carried out with PalmSenspotentiostat (Palm Instrument BV) connected to a laptop (Hewlett-Packard running windows 10). The software PS trace Master 4 was used for the execution of command. The electrochemical cell consists of conventional three-electrode system. The working electrode was a bare CPE or a poly(Eriochrome blue back R)-CPE, the counter electrode was a platinum wire and a silver-silver chloride electrode (Ag/AgCl) was employed as reference electrode.

### 2.2. Reagents and material

All chemicals used for the preparation of the stock and standard solutions were analytical grade. Graphite powder (99.9995%) was purchased by Alfa Aesar. Paraffin oil and Eriochrome blue black R, ( $\text{C}_{20}\text{H}_{13}\text{N}_2\text{NaO}_5\text{S}$ , scheme 1) were obtained from Sigma-Aldrich. EBB R solution was prepared by dissolving 0.4163 g of EBB R in 100 mL of absolute ethanol. Stock solution  $1 \times 10^{-2} \text{ mol.L}^{-1}$  of  $\text{Hg}^{2+}$  were prepared by dissolving 0.271 g of mercury chloric  $\text{HgCl}_2$ , (Merck KGaA) in 100 mL of  $\text{HClO}_4$  0.1  $\text{mol.L}^{-1}$  solution. More diluted mercury standards ( $1 \times 10^{-4} \text{ mol.L}^{-1}$ ,  $1 \times 10^{-5} \text{ M}$ ,  $1 \times 10^{-6} \text{ mol.L}^{-1}$ ) were prepared from this stock solution. Some ions used in interference studies  $\text{Pb}^{2+}$ ,  $\text{Cd}^{2+}$ ,  $\text{Cu}^{2+}$ ,  $\text{Cl}^-$  and  $\text{CN}^-$  were prepared respectively from lead chloride,  $\text{Pb}(\text{Cl})_2$  (Merck Schuchardt OHG)  $m = 0.2781 \text{ g}$ ; zinc chloride,  $\text{Zn}(\text{Cl})_2$  (Alfa Aesar)  $m = 0.1390 \text{ g}$ ; cadmium chloride,  $\text{Cd}(\text{Cl})_2$  (Alfa Aesar)  $m = 0.1833 \text{ g}$ ; copper chloride,  $\text{Cu}(\text{Cl})_2$  (Alfa Aesar)  $m = 0.13 \text{ g}$ ; potassium chloride, KCl (Merck KGaA)  $m = 0.0075 \text{ g}$  and potassium cyanide, KCN (Merck KGaA)  $m = 0.0651 \text{ g}$ . These different solutions are prepared in the same way: the weights are dissolved in 100 mL of distilled water to have a final concentration of  $1 \times 10^{-3} \text{ mol.L}^{-1}$ .

### 2.3. Sample preparation

Tap water samples were collected from the laboratory. The well water sample was collected in the city of Niamey (Capital of Niger). Water samples were collected in 1000 mL polyethylene bottles.

### 2.4. Preparation of carbon paste electrode

The bare CPE was prepared by mixing 2 g of graphite powder and 0.76 mL of paraffin oil in a mortar using a pestle. The mixture was carried out until a homogenous paste was obtained. Once homogeneity was observed, the mixed paste was then inserted into the cylindrical cavity of the body of carbon paste electrode (ID 2.87 mm) and polished on smooth

paper. The polished electrode was rinsed with distilled water to wash away polish residue, and finally put into the electrochemical cell.

## 2.5. Electropolymerization of the monomer on carbon paste electrode

As it has been reported by Genget al. [21], electropolymerization is more favorable in alkaline medium for the deposition than acidic because of the large amount of proton loss in acidic medium. So, the electropolymerization of Eriochrome Blue Black R (EBB R) was done similarly to literature [16]. It was carried out in 0.1 mol.L<sup>-1</sup> NaOH solution containing 3x10<sup>-4</sup> mol.L<sup>-1</sup> Eriochrome blue black R by cyclic voltammetry. The potential was scanned between -0.4 and +1 V at a sweep rate of 100 mV.s<sup>-1</sup> for 25 cycles. After polymerization, the electrode was rinsed with distilled water and placed in the electrochemical cell for further use.

## 2.6. Differential pulse anodic stripping voltammetric (DPASV) measurement of Hg<sup>2+</sup> at the modified electrode

The poly(EBB R)-CPE was immersed in aqueous solution containing 2.5x10<sup>-4</sup> mol.L<sup>-1</sup> Hg<sup>2+</sup> in 0.1 mol.L<sup>-1</sup> KCl made by dissolving 3.73 g in 500 mL of distilled water. The preconcentration of Hg<sup>2+</sup> was carried out under open circuit and in stirred solution. After the preconcentration step was completed, stirring was stopped and a 30 s rest period was used to allow the solution to become quiescent. Then the voltammogram was scanned from -0.4 V to 1 V using DPASV. The parameters of differential pulse voltammetry used were a potential step height of 10 mV, pulse amplitude of 50 mV and duration of 50 ms. The same procedure was used for bare CPE and poly(EBB R)-CPE.

## 3. RESULTS AND DISCUSSION

### 3.1. Electropolymerization of Eriochrome blue black R (EBB R) on the surface of carbon paste electrode

The cyclic voltammograms during the electropolymerization of Eriochrome blue black R are shown in Fig. 1. Eriochrome blue black R was electropolymerized on the working electrode surface by scanning the potential from -0.4 to 1 V at a scan rate of 100 mV.s<sup>-1</sup> for 25 cycles in 0.1 mol.L<sup>-1</sup> NaOH. During the first scan, a well-defined anodic peak (Pa<sub>1</sub>) and cathodic peak (Pc<sub>1</sub>) were observed at -0.02 V/0.394 μA and -0.07 V/ -0.137 μA, respectively. These peaks show that there is an exchange of electrons at the interface electrode/electrolyte. The anodic peak is due to the oxidation of the monomer which initiates the polymerization [21]. From the 1<sup>st</sup> scan to the 2<sup>nd</sup> scan, there is a large drop in the intensity of the anodic peak. The anodic and cathodic peaks decrease gradually during successive scans, and tend to become stable after 25 scans. Guha et al. [16] and Yao et al. [17], made the same observation during the electropolymerization of Eriochrome black T, and reported that such a decrease indicates the formation and deposition of the polymer film on the surface of the electrode. Eriochrome blue black R, like other dyes, is a very electron-rich compound. Therefore, it is difficult to present a detailed mechanism for the electropolymerization of it. Thus, in the literature the authors limit themselves to a simple mechanism. Based on what Guha et al. [16] and Yao et al. [17], reported, the polymerization of EBB R (structure a, Scheme 1) forms benzoquinone diimine (structure b, Scheme 1) which is then reduced back to EBB R on the surface of the electrode. The mechanism is shown in Scheme 1.

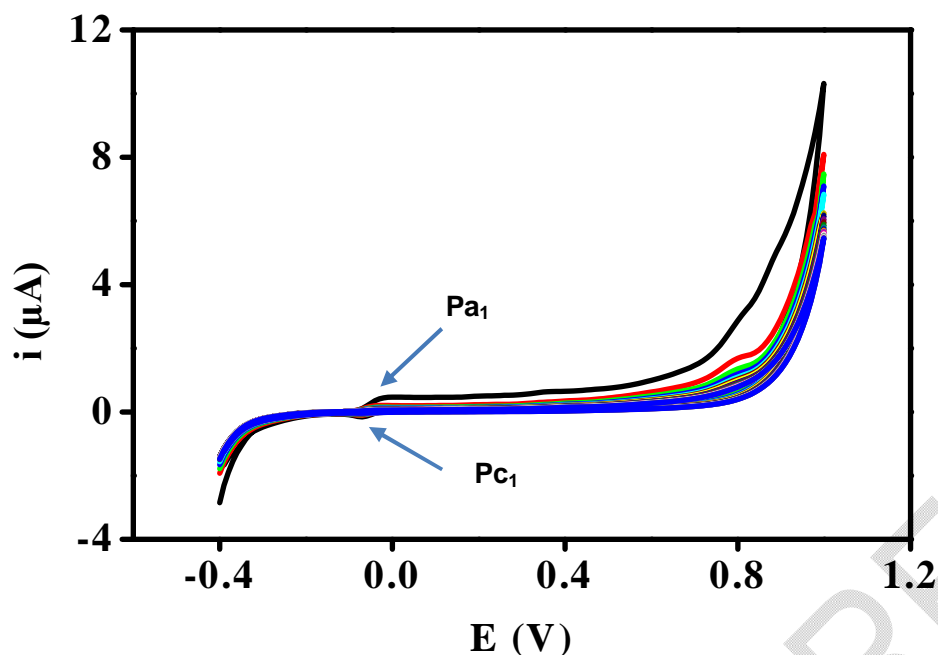
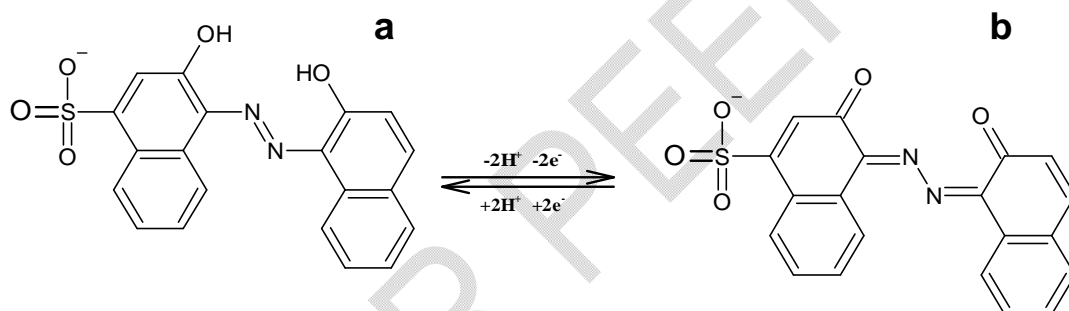


Fig. 1. Cyclic voltammograms recorded for the polymerization of Eriochrome blue black R at the carbon paste electrode in 0.1 mol.L<sup>-1</sup> of NaOH containing 300 μmol.L<sup>-1</sup> of monomer during 25 cycles. Scan rate, 100 mV.s<sup>-1</sup>



Scheme 1. Mechanism of polymerization of Eriochrome blue black R

### 3.2. Characterization by electrochemical impedance spectroscopy (SIE)

The surface morphology of CPE-modified with poly(EBB R) was characterized by SIE. The Nyquist plots of the bare carbon paste electrode (black curve) and the carbon paste electrode modified with poly(EBB R) (red curve) in the supporting electrolyte of 1 mol.L<sup>-1</sup> KCl containing 1 mmol.L<sup>-1</sup> of the complex [Fe(CN)<sub>6</sub>]<sup>3-/4-</sup> are shown in Fig. 2. The two curves describe a semicircle and a straight line. In general, the semicircle in the higher frequency is characteristic of the highest charge transfer resistance and the straight line at low frequency is due to the diffusion limiting process [22]. The charge transfers resistance (R<sub>ct</sub>) of the bare carbon paste electrode and the carbon paste electrode modified with poly(EBB R) are 15 kΩ and 5 kΩ, respectively. According to Salih et al. [23], the decrease in the R<sub>ct</sub> observed during the modification of the poly(EBB R) modified-CPE shows that the polymer (poly(EBB R)) was effectively carried out and significantly increase the electron transfer at the electrode surface because of the electronic properties of the polymer.

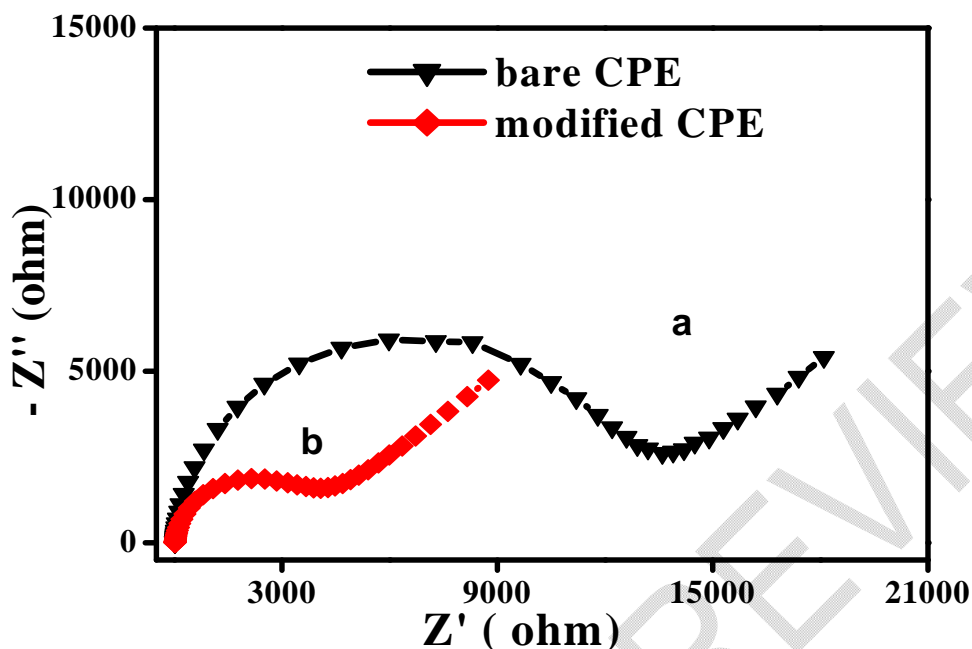


Fig. 2. Nyquist plots for different electrodes in  $1 \text{ mmol.L}^{-1}$  of  $[\text{Fe}(\text{CN})_6]^{3-/4-}$  containing  $1 \text{ mol.L}^{-1}$  KCl: a. bare carbon paste electrode; b. modified poly(EBB R)-carbon paste electrode

### 3.3. Electrochemical behavior of $\text{Hg}^{2+}$ ions at the bare carbon paste and modified poly(Eriochrome blue black R)-carbon paste electrode

#### 3.3.1. Characterization by cyclic voltammetric

Cyclic voltammograms of bare CPE and modified poly(EBB R)-CPE in  $1 \text{ mol.L}^{-1}$  KCl for the detection of  $2.5 \times 10^{-4} \text{ mol.L}^{-1}$  of  $\text{Hg}^{2+}$  are illustrated in Fig. 3. It can be seen that no peak (green curve) is displayed at the bare CPE in the absence of  $\text{Hg}^{2+}$ . But in the presence of  $\text{Hg}^{2+}$  (red curve) a weak peak anodic  $0.070 \text{ V}/6.25 \mu\text{A}$  is observed then a crossing between the anodic branch and cathodic branch. Moreover, when the modified poly(EBB R)-CPE is immersed in the solution in presence of  $\text{Hg}^{2+}$  (black curve) the signal at  $0.070 \text{ V}$  increased to  $20.38 \mu\text{A}$ , which was more intense than the bare CPE, then two crossings between the anodic and cathodic branches. The crossings over indicate a nucleation and growth phenomenon. The bare CPE has the difficulty of preconcentration the  $\text{Hg}^{2+}$  ions in the solution while the modified CPE by the film polymer significantly increased the intensity of the current, showing easier charge transfer on the surface of the polymer film.

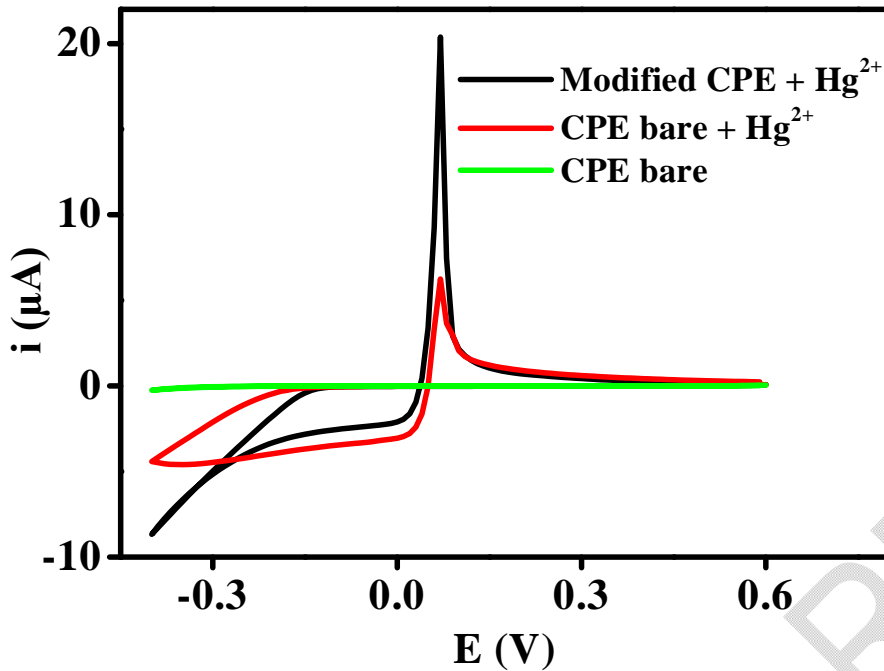
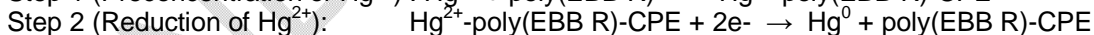
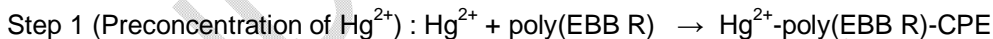


Fig. 3. Cyclic voltammograms obtained at: a. bare CPE, b. bare CPE containing  $2.5 \times 10^{-4} \text{ mol.L}^{-1} \text{ Hg}^{2+}$  and c. poly(EBB R)-CPE containing  $2.5 \times 10^{-4} \text{ mol.L}^{-1} \text{ Hg}^{2+}$  in  $1 \text{ mol.L}^{-1} \text{ KCl}$ ; Scan rate 50 mV/s

### 3.3.2. Determination of $\text{Hg}^{2+}$ by differential pulse anodic stripping voltammetry

Preliminary studies of mercury accumulation were carried out by recording the Differential Pulse Anodic Stripping Voltammograms on a bare carbon paste electrode and on the MCPE.

Firstly, the study of the behavior of the bare carbon paste electrode and the modified polymer film-CPE in the supporting electrolyte  $0.1 \text{ mol.L}^{-1} \text{ KCl}$  were illustrated in Fig. 4. It can be seen that no oxidation peak (black and blue curve) is observed for bare CPE and modified polymer film-CPE in the absence of  $\text{Hg}^{2+}$  proving that the solution isn't contaminated. When  $\text{Hg}^{2+}$  was added in the same solution ( $0.1 \text{ mol.L}^{-1} \text{ KCl}$ ) under the same conditions at the bare CPE (green curve) and modified polymer film-CPE (red curve), an anodic redissolution peak was observed at  $0.088 \text{ V}/2.38 \mu\text{A}$  and  $0.092 \text{ V}/20.34 \mu\text{A}$ , respectively. These results show that the best response is provided by the modified CPE, and it is 8.5 times more intense than the bare CPE. The peak is well resolved and will serve for the determination of inorganic mercury in aqueous medium. The following reactions may take place at the surface of the electrode [24]:



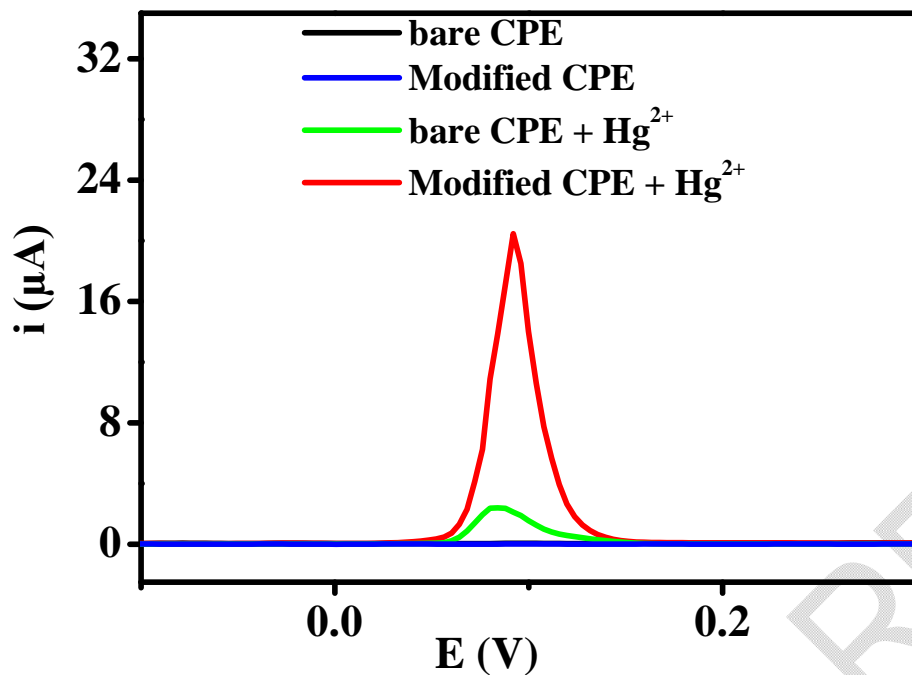


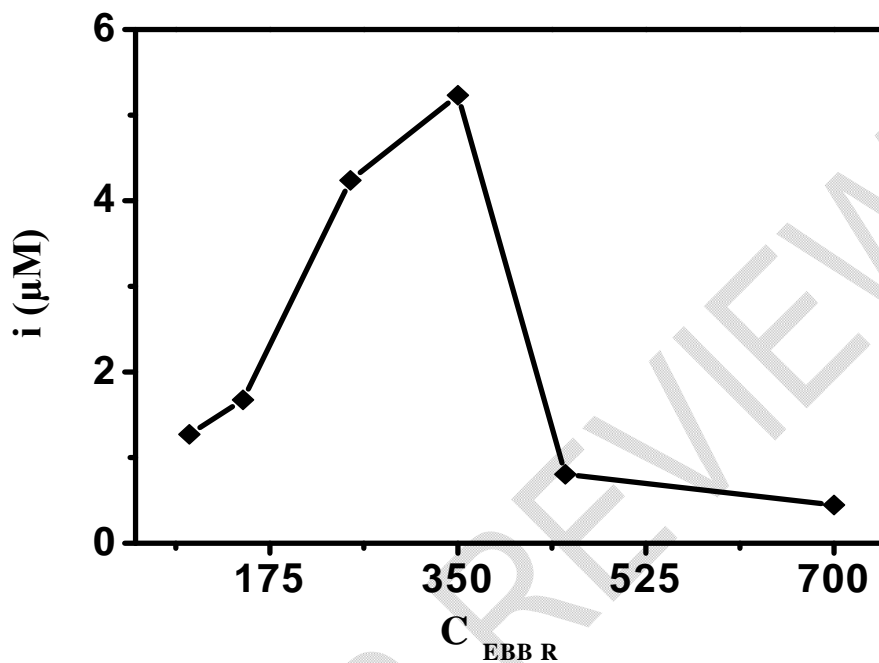
Fig. 4. DPASV of bare CPE (a), modified poly(EBB R)-CPE (b), bare CPE in the presence of  $2.5 \times 10^{-4} \text{ mol.L}^{-1} \text{ Hg}^{2+}$  (c), modified poly(EBB R)-CPE in presence of  $2.5 \times 10^{-4} \text{ mol.L}^{-1} \text{ Hg}^{2+}$  (d), in  $0.1 \text{ mol.L}^{-1} \text{ KCl}$ ; scan rate  $20 \text{ mV/s}$ ; deposition time  $120 \text{ s}$ ; pulse amplitude  $50 \text{ mV}$

### 3.4. Optimization of analytical parameters

#### 3.4.1. Effect of concentration of Eriochrome blue black R

The effect of concentration of Eriochrome blue black R during the electropolymerization has been studied between  $100$  and  $700 \text{ } \mu\text{mol.L}^{-1}$ . As shown in Fig. 5, the intensity of the peak current of  $\text{Hg}^{2+}$  oxidation increase according to the concentration of EBB R from  $100 \text{ } \mu\text{mol.L}^{-1}$  to  $350 \text{ } \mu\text{mol.L}^{-1}$ . The increase in the intensity of the current is explained by the increase of monomer on the surface of carbon paste to form more polymer and therefore more sites available to accumulate  $\text{Hg}^{2+}$ . Increasing the concentration of EBB R beyond  $350 \text{ } \mu\text{mol.L}^{-1}$  decreased the sensitivity of  $\text{Hg}^{2+}$  determination by the modified poly(EBB R)-CPE. According to several authors, such as Dueraning et al. [25], this was probably because the polymer became too thick and blocked the electrical conductivity. Moreover, there are some oxidation peaks appearing in cyclic voltammograms which lead us to the decrease in the intensity of the current. These

new oxidation peaks could be due to the appearance of new sites to capture the inorganic mercury present in the solution



during the first step of DPASV.

**Fig. 5. Effect of the variation of the EBB R (Calcon) concentration on the peak current intensity by DPASV.  $[\text{Hg}^{2+}]$   $35 \mu\text{mol.L}^{-1}$ ; scanning speed 20 mV/s; deposition time 120 s; pulse amplitude 50 mV.**

### **3.4.2. Effect of supporting electrolyte**

The differential pulse voltammograms of  $35 \mu\text{mol.L}^{-1}$  of  $\text{Hg}^{2+}$ , carried out in  $0.1 \text{ mol.L}^{-1}$  of KCl,  $\text{NH}_4\text{Cl}$ ,  $\text{KNO}_3$ , KCl,  $\text{NH}_4\text{Cl}$ , acetate buffer solution (ABS) (pH=4.22) and phosphate buffer solution (PBS) (pH= 6.68), are illustrated in Fig. 6. The optimum response was observed in  $\text{HClO}_4$  medium and this electrolyte was chosen as the supporting electrolyte for the remaining experiments. The high intensity of the current in  $\text{HClO}_4$ , is explained by the fact that it is an acid in which the mercury chloride ( $\text{HgCl}_2$ ) has a high solubility, allowing to have the specie  $\text{Hg}^{2+}$  in solution.

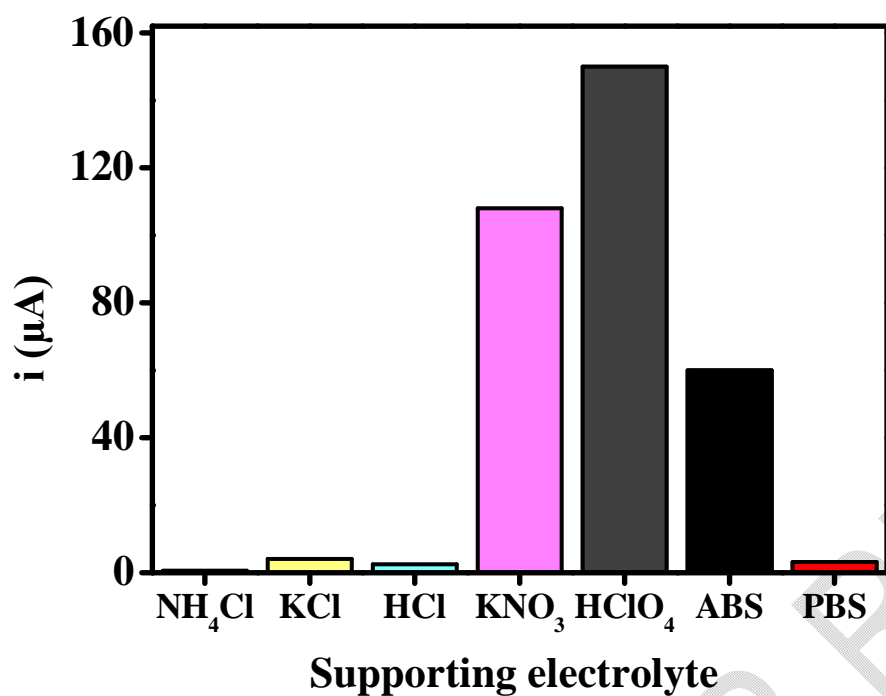


Fig. 6. Effect of supporting electrolyte on DPASV peak current for the determination of  $35\mu\text{mol.L}^{-1}$   $\text{Hg}^{2+}$

### 3.4.3. Effect of the concentration of supporting electrolyte

The effect of the concentration of  $\text{HClO}_4$  can be seen in Fig. 7. The intensity of the current increases depending on the concentration of the supporting electrolyte from 0.1 to 0.8  $\text{mol.L}^{-1}$ , and decreases after 0.8  $\text{mol.L}^{-1}$ . Therefore, 0.8  $\text{mol.L}^{-1}$  of  $\text{HClO}_4$  was used for further experiments.

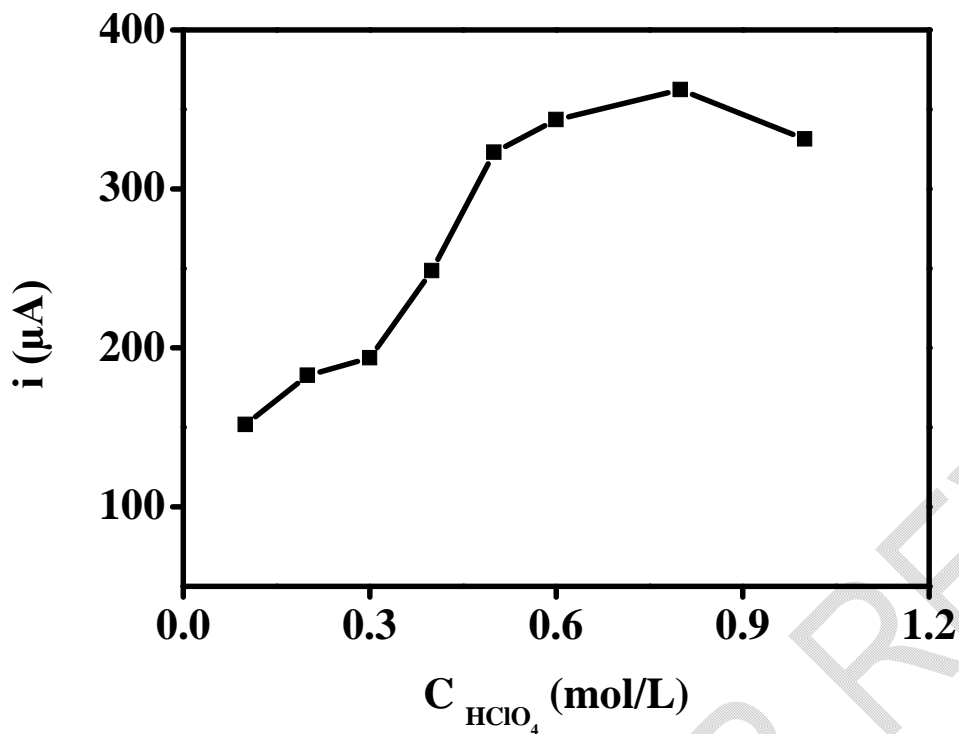


Fig. 7. Effect of concentration of  $\text{HClO}_4$  on DPASV peak current for the determination of  $35 \mu\text{mol.L}^{-1} \text{Hg}^{2+}$

#### 3.4.4. Effect of deposition potential

Deposition potential is an important parameter for stripping techniques and has a significant effect on the sensitivity [26]. Fig. 8 shows a significant increase in intensity as a function of the deposition potential of the current down to  $-350 \text{ mV}$ . Over this potential, the intensity of the peak decreases. So, the deposition potential of  $-350 \text{ mV}$  was taken as the optimal potential for  $\text{Hg}^{2+}$  deposition on the surface of the modified electrode.

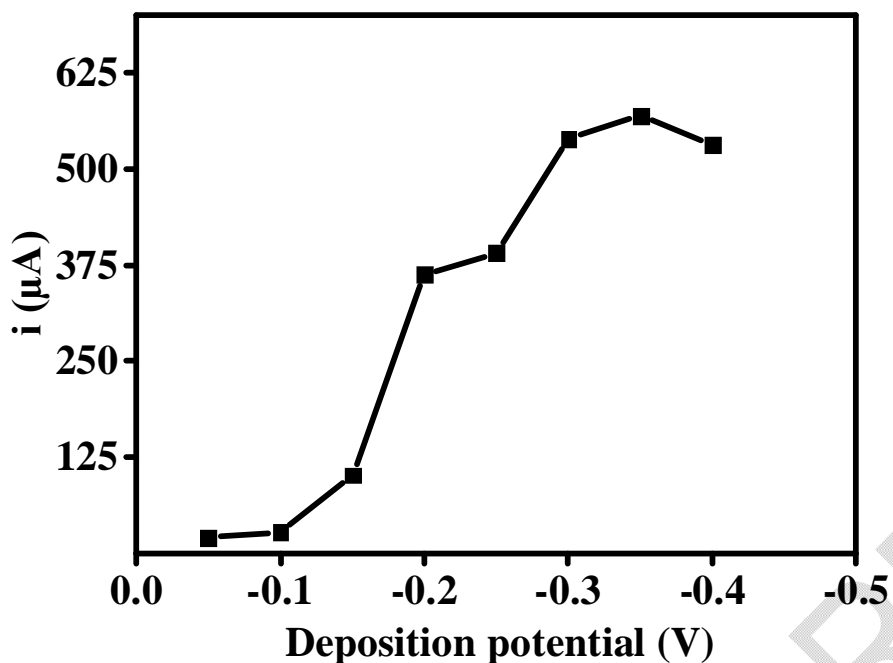


Fig. 8. Effect of the variation of the deposition potential on the peak current intensity by DPASV.  $[\text{Hg}^{2+}]$  35  $\mu\text{mol.L}^{-1}$ ; scan rate 20 mV/s; pulse amplitude 50 mV; stirring speed 400 rpm

### 3.4.5. Effect of deposition time

Fig. 9 illustrated the effect of deposition time on the current intensity in the range of 0 to 240 s. It is seen that the peak current increases with the deposition time from 0 to 120 s. While, the peak current was decreased with further the deposition potential after 120s. The decrease is due to the saturation of mercury on the surface of the electrode. Therefore, 120 seconds was chosen as optimal deposition time.

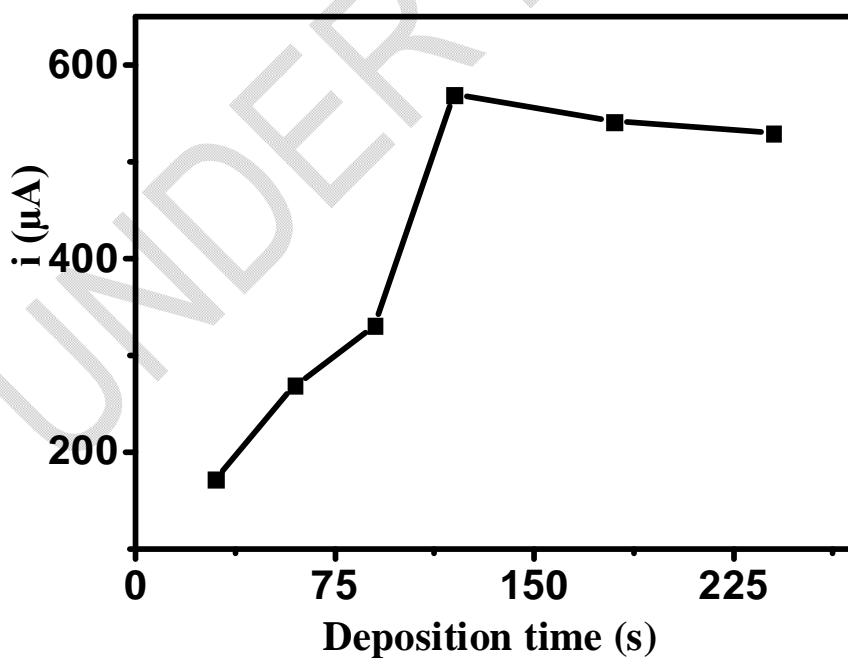


Fig. 9. Effect of the variation of the deposition time on the peak current intensity by DPASV.  $[\text{Hg}^{2+}]$   $35\mu\text{mol.L}^{-1}$ ; scan rate  $20\text{ mV/s}$ ; deposition potential  $-0.35\text{V}$ ; pulse amplitude  $50\text{ mV}$ ; stirring speed  $400\text{ rpm}$

### 3.4.6. Effect of mechanical stirring of the solution

Stirring the solution during voltammetric measurements will give an increase in signal due to a better mass transport to the electrode corresponding to an effective decrease in the thickness of the diffusion layer [27]. Mechanical stirring speeds, between  $200$  and  $700\text{ rpm}$  (revolution per minutes), were applied in the mercury deposition step. Results are shown in Fig. 10. The intensity of the peak current increases linearly with the increase of the stirring speed up to  $600\text{ rpm}$ , but dropped at  $700\text{ rpm}$ . According to several authors such as [28], this decrease could be attributed to more distribution of the solution that could perturb the deposition step. At  $600\text{ rpm}$ , the highest current peak is obtained, but  $400\text{ rpm}$  was selected for further experiments because the best reproducibility of the measurements was found at this stirring speed.

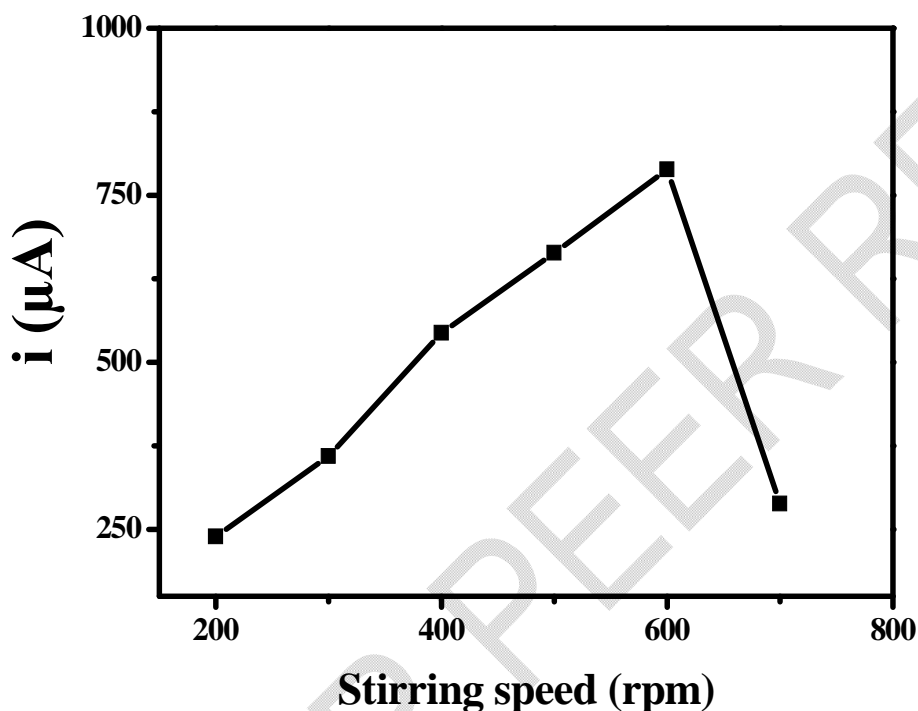


Fig. 10. Effect of mechanical stirring speed on peak current intensity by DPASV.  $[\text{Hg}^{2+}]$   $35\mu\text{mol.L}^{-1}$ ; scan rate  $20\text{ mV/s}$ ; deposition time  $120\text{ s}$ ; pulse amplitude  $50\text{ mV}$

### 3.4.7. Optimization of DPV parameters

The influence of various parameters of DPV such as potential step, pulse amplitude, pulse time and scan rate were investigated in order to achieve high sensitivity for trace  $\text{Hg}^{2+}$  determination with the modified electrode. The potential step was varied from  $1$  to  $8\text{ mV}$ . As illustrated in Fig. 11.a, the maximum current intensity was found at  $4\text{ mV}$ . Fig. 11.b shows the effect of the pulse amplitude on the current intensity in the range of  $30$  and  $80\text{ mV}$ . The optimal pulse amplitude was at  $80\text{ mV}$ . As shown in Fig. 11.c the variation of pulse time on the current intensity was studied from  $10$  to  $50\text{ ms}$ . The optimal pulse time was found at  $30\text{ ms}$ . Finally, for the variation of scan rate, investigated in Fig. 11.d, the optimal value was  $20\text{ mV.s}^{-1}$ .

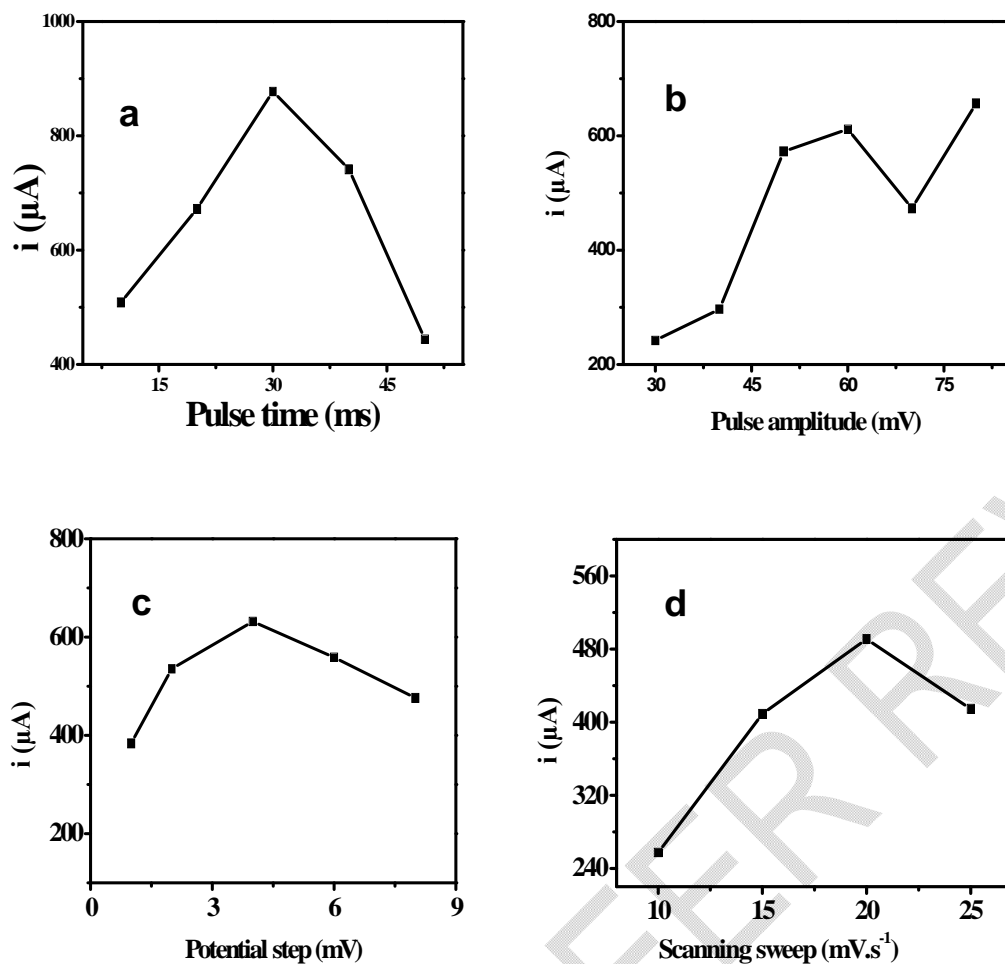


Fig. 11. Influence of DPV parameters (a. Pulse time; b. Pulse amplitude; c. Potential step; and d. Scanning sweep) on the peak current intensity by DPASV for determination of  $35 \mu\text{mol}\cdot\text{L}^{-1} \text{Hg}^{2+}$  in  $0.8 \text{mol}\cdot\text{L}^{-1} \text{HClO}_4$

### 3.4.8. Calibration plot

Fig. 12 presents the differential pulse voltammograms of various concentrations of  $\text{Hg}^{2+}$  in the range of 0 to  $9 \times 10^{-9} \text{mol}\cdot\text{L}^{-1}$ , with the poly(EBB R)-CPE. It was observed that the peak currents increase linearly with the increased concentration of  $\text{Hg}^{2+}$  in the range studied, and the corresponding linear regression equation was  $I_{pa} (\mu\text{A}) = 1.479 \cdot 10^8 [\text{Hg}^{2+}] - 0.00656$  with a correlation coefficient ( $R^2$ ) of 0.9987. The limit of detection (LOD) and the limit of quantification (LOQ), calculated in the concentration range of  $1 \times 10^{-9}$  to  $9 \times 10^{-9} \text{mol}\cdot\text{L}^{-1}$  are respectively  $3.23 \times 10^{-10} \text{mol}\cdot\text{L}^{-1}$  and  $1.07 \times 10^{-9} \text{mol}\cdot\text{L}^{-1}$ . The relative standard deviation (RSD) for seven repetitions analysis in  $0.8 \text{mol}\cdot\text{L}^{-1}$  of  $\text{HClO}_4$  containing  $5 \times 10^{-9} \text{mol}\cdot\text{L}^{-1} \text{Hg}^{2+}$  by DPASV was 3.07%.

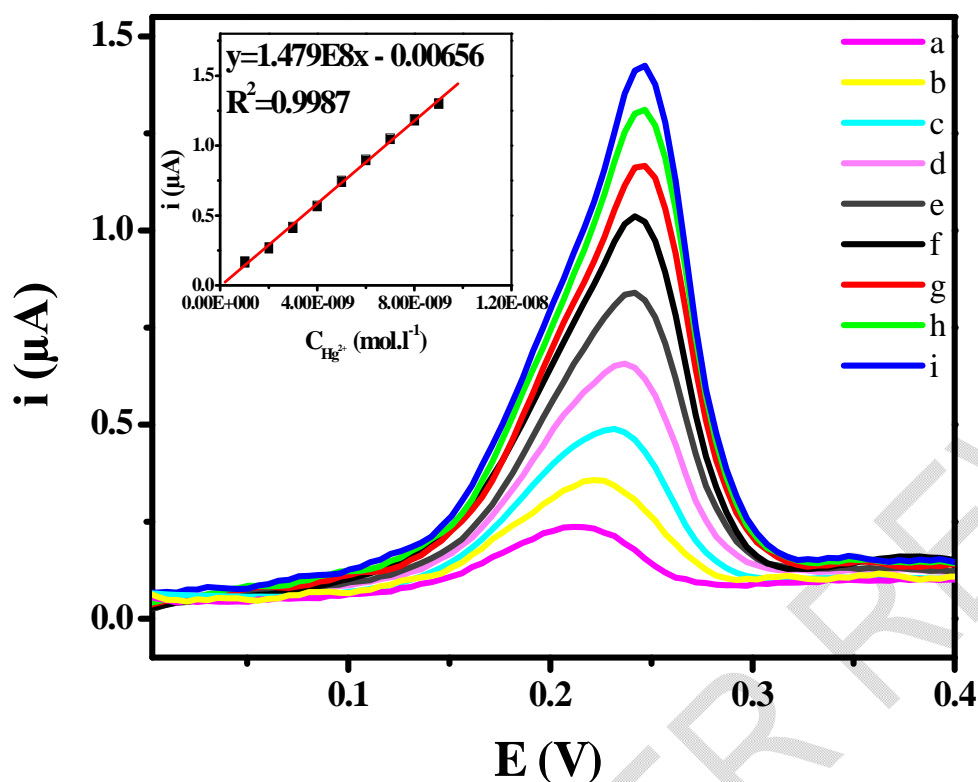


Fig. 12. DPASV of various concentrations of  $Hg^{2+}$  to 0 to  $9 \times 10^{-9} mol.L^{-1}$ : b)  $1 \times 10^{-9} mol.L^{-1}$ , c)  $2 \times 10^{-9} mol.L^{-1}$ , d)  $3 \times 10^{-9} mol.L^{-1}$ , e)  $4 \times 10^{-9} mol.L^{-1}$ , f)  $5 \times 10^{-9} mol.L^{-1}$ , g)  $6 \times 10^{-9} mol.L^{-1}$ , h)  $7 \times 10^{-9} mol.L^{-1}$ , i)  $8 \times 10^{-9} mol.L^{-1}$ , j)  $9 \times 10^{-9} mol.L^{-1}$

Table 1 shows the comparison of the modified poly(Eriochrome blue black R)-CPE presented in this work with other electrodes reported in the literature for the detection of  $Hg^{2+}$ . This comparison is based on the relative standard deviation (RSD) and LOD of the different sensors. As can be seen in the Table 1, this method showed a low detection limit and satisfactory RSD. This proves that the sensor developed in this work is sensitive, efficient, and can be used for trace level analysis of  $Hg^{2+}$  in aqueous media.

Table 1. Comparison of modified poly(Eriochrome blue black R)-CPE with other modified CPE developed for the determination of  $Hg^{2+}$

Electrodes	Technique	LOD ( $mol.L^{-1}$ )	RSD	Accumulation time (s)	Reference
poly(Eriochrome blue black R)/CPE	DPASV	$3.23 \times 10^{-10}$	3.07 % for 7 measurements	120	Present work
poly(Eriochrome black T)/CPE	DPASV	$2.20 \times 10^{-10}$	2.4 % for 6 measurements	120	[Error! Reference source not found.]
poly(glycine)/GPE	DPV	$6.60 \times 10^{-6}$	/	/	[Error! Reference source not found.]
EDTA/CPE	SWV	$8.6 \times 10^{-9}$	3.1 % for 7 measurements	300	[Error! Reference source not found.]

12-Crown Ether/MWCNTs/CPE	LS-AdSV	$1.25 \times 10^{-10}$	5 % for 10 measurements	/	found.] [Error! Reference source not found.]
5-Br-PADAP/CPE	DPV	$1 \times 10^{-8}$	1.6 % for 10 measurements	120	found.] [Error! Reference source not found.]

### 3.4.9. Interference studies

The presence of certain ions such as  $\text{Cd}^{2+}$ ,  $\text{Cu}^{2+}$ ,  $\text{Zn}^{2+}$ ,  $\text{Pb}^{2+}$ ,  $\text{CN}^-$  and  $\text{Cl}^-$  are listed in gold mining sites that can affect the determination of inorganic mercury using CPE-modified with poly(Eriochrome blue black R). The presence of these ions was examined for the determination of  $1 \times 10^{-8} \text{ mol.L}^{-1}$   $\text{Hg}^{2+}$  using the optimal conditions described above. The experimental results illustrated at Table 2 show the response of the modified electrode is not remarkably disturbed ( $\text{Cd}^{2+}$ ,  $\text{Cu}^{2+}$  and  $\text{Zn}^{2+}$ ) but some ions such as  $\text{CN}^-$  interfere when they had a 10 fold excess in the analyte solution. For the  $\text{CN}^-$ , this could be due to his strong affinity towards  $\text{Hg}^{2+}$  at the surface of the electrode (ability of  $\text{CN}^-$  to complex the  $\text{Hg}^{2+}$ ) [31]. An increase in current is observed for  $\text{Pb}^{2+}$ , and  $\text{Cl}^-$  ions when their concentration is 10 fold that of  $\text{Hg}^{2+}$ . The matrix effect is minimized, during measurements on real samples, using the standard addition technique.

**Table 2. Interference of some ions with the determination of  $1 \times 10^{-8} \text{ mol.L}^{-1}$  of  $\text{Hg}^{2+}$  at poly(EBB R)-CPE**

	Current intensity(1 fold)	Current variation	Current intensity (10 fold)	Current variation
$\text{Hg}^{2+}$	$0.3125 \pm 0.06$			
$\text{Cd}^{2+}$	$0.3226 \pm 0.03$	+ 0.03 %	$0.354 \pm 0.05$	+ 0.13%
$\text{Cu}^{2+}$	$0.311 \pm 0.01$	- 0.004 %	$0.276 \pm 0.006$	- 11.6%
$\text{Zn}^{2+}$	$0.289 \pm 0.05$	- 7.3 %	$0.282 \pm 0.03$	- 9.8%
$\text{CN}^-$	$0.292 \pm 0.009$	- 6.4%	$0.145 \pm 0.01$	- 53.4%
$\text{Cl}^-$	$0.249 \pm 0.04$	- 3.42 %	$0.423 \pm 0.02$	+ 35%
$\text{Pb}^{2+}$	$0.345 \pm 0.02$	+ 10 %	$0.415 \pm 0.03$	+ 32%

### 3.4.10. Analytical applications

In order to evaluate the analytical applicability of the proposed method, known concentrations of Hg was introduced into samples and determined by the standard addition method using the optimal parameters described. The results of the recovery data of different concentrations in distilled water and well water obtained (Table 3) are between 98.71 and 100.38% which are very satisfactory. Thus, the sensor poly(EBB R)-CPE developed is very suitable for the determination of trace of mercury  $\text{Hg}^{2+}$  ions in aqueous media.

**Table 3. Recovery data for  $\text{Hg}^{2+}$  obtained for distilled water and well water**

Samples	$[\text{Hg}^{2+}]$ Spiked ( $\mu\text{mol.L}^{-1}$ )	$[\text{Hg}^{2+}]$ Founded ( $\mu\text{mol.L}^{-1}$ )	Recovery (%)
Distilled water	0.002	0.00198	98.76
	0.005	0.005019	100.38
	0.0075	0.007404	98.71
Well water	0.005	0.00496	99.2
	0.05	0.05005	100.1

## 4. CONCLUSION

In this work, we reported a new sensitive and efficient sensor using poly(Eriochrome blue black R)-CPE for the determination of  $\text{Hg}^{2+}$  in aqueous medium. Cyclic voltammetry and electrochemical impedance spectroscopy show a well deposited film polymer on the surface of carbon paste. After optimization of analytical parameters, the sensor has a linear dynamic range, a low limit of detection, a good reproducibility and application of this sensor in real samples were satisfactory.

## REFERENCES

1. Liao Y, Li J, Li S, Han B, Wu P, Deng N et al. Inorganic mercury induces liver oxidative stress injury in quails by inhibiting Akt/Nrf2 signal pathway, *Inorg. Chem. Commun.* 2022;142: 109603.DOI: <https://doi.org/10.1016/j.inoche.2022.109603>
2. Ganguly J, Kulshreshtha D, Jog M.Mercury and Movement Disorders: The Toxic Legacy Continues.*Can. J. Neurol. Sci.* 2022;49 :493 – 501.DOI: <https://doi.org/10.1017/cjn.2021.146>
3. NunesPBdO, Ferreira MKM, Frazão DR, Bittencourt LO, ChemeloVdS., Silva MCF et al.Effects of inorganic mercury exposure in the alveolar bone of rats: an approach of qualitative and morphological aspects.*PeerJ.*2022;10 :12573.DOI: <https://doi.org/10.7717/peerj.12573>
4. Li S, Han B, Wu P, Yang Q, Wang X, Li J et al.Effect of inorganic mercury exposure on reproductive system of male mice: Immunosuppression and fibrosis in testis,*Environ. Toxicol.* 2022;37: 69-78. DOI: <https://onlinelibrary.wiley.com/doi/epdf/10.1002/tox.23378>
5. Han B, Lv Z, Han X, Li S, Han B, Yang Q et al.Harmful Effects of Inorganic Mercury Exposure on Kidney Cells: Mitochondrial Dynamics Disorder and Excessive Oxidative Stress.*Biol. Trace Elem. Res.* 2022;200:1591–1597.DOI: <https://doi.org/10.1007/s12011-021-02766-3>
6. Tian J, Zhu Y. Rapid Determination of Mercury Ions in Environmental Water Based on an N-Rich Covalent Organic Framework Potential Sensor.*Int. J. Chem. Eng.*2022;2022:3112316.DOI: <https://doi.org/10.1155/2022/3112316>
7. Cossa D, Knoery J, Bănaru D, Harmelin-Vivien M, Sonke JE, Hedgecock IM et al.Mediterranean Mercury Assessment 2022: An Updated Budget, Health Consequences, and Research Perspectives.*Environ. Sci. Technol.* 2022;56(7): 3840–3862.DOI: <https://doi.org/10.1021/acs.est.1c03044>
8. Che S, Yin L, Fan Y, Shou Q, Zhou C, Fu H, She Y.An ionic liquid-based ratio fluorescent sensor for real-time visual monitoring of trace  $\text{Hg}^{2+}$ . *Sens. Actuators B Chem.*2022;360(1):131588.DOI: <https://doi.org/10.1016/j.snb.2022.131588>
9. Wang Y, Zhu A, Fang Y, Fan C, Guo Y, Tan Z, et al.Dithizone-functionalized C18 online solid-phase extraction-HPLC-ICP-MS for speciation of ultra-trace organic and inorganic mercury in cereals and environmental samples.*J. Environ. Sci.*2022;115:403–410. DOI: <https://doi.org/10.1016/j.jes.2021.08.013>
10. Yang H, Jian R, Liao J, Cui J, Fang P, Zou Z, Huang K.Recent development of non-chromatographic atomic spectrometry for speciation analysis of mercury.*Appl. Spectrosc. Rev.*2021;57:441-460DOI: <https://doi.org/10.1080/05704928.2021.1893183>
11. Ali S, Mansha M, Baig N, Khan SA.Cost-Effective and Selective Fluorescent Chemosensor (Pyr-NH@SiO<sub>2</sub> NPs) for Mercury Detection in Seawater.*Nanomaterials.*2022;12:1249. DOI: <https://doi.org/10.3390/nano12081249>
12. Liu Q, Wu F, Di H, Bi Y, Meng M, Liu D et al.A novel SERS biosensor for ultrasensitive detection of mercury(II) in complex biological samples.*Sens. Actuators B Chem.* 2022;351:130934.DOI: <https://doi.org/10.1016/j.snb.2021.130934>
13. Mahamane AA, Despas C, Adamou R, Walcarius A.Carbon paste electrode modified with 5-Br-PADAP as a new electrochemical sensor for the detection of inorganic mercury(II).*J. Mater. Environ. Sci.*, 2022;13(01):54-69.[https://www.jmaterenvironsci.com/Document/vol13/vol13\\_N1/JMES-2022-13005-Mahamane.pdf](https://www.jmaterenvironsci.com/Document/vol13/vol13_N1/JMES-2022-13005-Mahamane.pdf)
14. Tajik S, Beitollahi H, Nejad FG, Dourandish Z, Khalilzadeh MA, H. W. Jang et al.Recent Developments in Polymer Nanocomposite-Based Electrochemical Sensors for Detecting Environmental Pollutants.*Ind. Eng. Chem. Res.*2021;60(03):1112–1136.DOI: <https://doi.org/10.1021/acs.iecr.0c04952>
15. Somerset V, Leaner J, Mason R, Iwuoha E, Morrin A. Development and application of a poly(2,2'-dithiodianiline) (PDTDA)-coated screen-printed carbon electrode in inorganic mercury determination.*Electrochim. Acta.* 2010;55 (14):4240-4246.DOI: <https://doi.org/10.1016/j.electacta.2009.01.029>
16. Guha KS, Mascarenhas RJ, Thomas T, D'Souza OJ.Differential pulse anodic stripping voltammetric determination of  $\text{Hg}^{2+}$  at poly(Eriochrome Black T)-modified carbon paste electrode.*Springer.*2014;20:849–856.DOI: <https://doi.org/10.1007/s11581-013-1040-9>
17. Yao H, Sun Y, Lin X, Tang Y, Liu A, Li G et al.Selective Determination of Epinephrine in the Presence of Ascorbic Acid and Uric Acid by Electrocatalytic Oxidation at Poly(eriochrome Black T) Film-modified Glassy Carbon Electrode.*Anal. Sci.* 2007;23 (6):677-682.DOI:<https://doi.org/10.2116/analsci.23.677>

18. RariilC, Manjunatha JG. Fabrication of novel polymer-modified graphene-based electrochemical sensor for the determination of mercury and lead ions in water and biological samples. *J. Anal. Sci. Technol.* 2020;11:3. DOI: <https://doi.org/10.1186/s40543-019-0194-0>
19. Tamer U, OymakT, Ertas N. Voltammetric Determination of Mercury(II) at Poly(3-hexylthiophene) Film Electrode. Effect of Halide Ions. *Electroanalysis.* 2007;19:2565 – 2570. DOI: <https://doi.org/10.1002/elan.200704013>
20. Zuo Y, Xua J, Zhua X, Duana X, Lub L, GaoaYet al. Poly(3,4-ethylenedioxythiophene) nanorods/graphene oxide nanocomposite as a new electrode material for the selective electrochemical detection of mercury (II). *Synth. Met.* 2016;220:14–19. DOI: <https://doi.org/10.1016/j.synthmet.2016.05.022>
21. Geng M, Xu J, Hu S. In situ electrogenerated poly(Eriochrome black T) film and its application in nitric oxide sensor. *React. Funct. Polym.* 2008;68:1253-1259. DOI: <https://doi.org/10.1016/j.reactfunctpolym.2008.06.001>
22. El Attar A, Chemchoub S, Kalan MD, OularbiL, El Rhazi M. Designing New Material Based on Functionalized Multi-Walled Carbon Nanotubes and Cu(OH)<sub>2</sub>-Cu<sub>2</sub>O/Polypyrrole Catalyst for Ethanol Oxidation in Alkaline Medium. *Front. Chem.* 2022;9:805654. DOI: <https://doi.org/10.3389/fchem.2021.805654>
23. Salih FE, Oularbi L, ElHalim, Elbasri M, Ouarzane A, El Rhazi M. Conducting Polymer/Ionic Liquid Composite Modified Carbon Paste Electrode for the Determination of Carbaryl in Real Samples. *Electroanalysis.* 2018;30(8):1855-1864. DOI: <https://doi.org/10.1002/elan.201800152>
24. Mariame C, El Rhazia M, Adraoui I. Determination of traces of copper by anodic stripping voltammetry at a rotating carbon paste disk electrode modified with poly(1,8-diaminonaphtalene). *J. Anal. Chem.* 2009;64:632–636. DOI: <https://doi.org/10.1134/S1061934809060161>
25. Dueraning A, Kanatharana P, Thavarungkul P, Limbut W. An environmental friendly electrode and extended cathodic potential window for anodic stripping voltammetry of zinc detection. *Electrochim. Acta*, 2016;221:133-143. DOI: <https://doi.org/10.1016/j.electacta.2016.10.069>
26. Bagheri H, Afkhami A, Khoshsafar H, Rezaei M, Shirzadmehr A. Simultaneous electrochemical determination of heavy metals using a triphenylphosphine/MWCNTs composite carbon ionic liquid electrode. *Sens. Actuators B.* 2013;186:451–460. DOI: <https://doi.org/10.1016/j.snb.2013.06.051>
27. Mikkelsen Ø, Schrøder KH. Sensitivity Enhancements in Stripping Voltammetry from Exposure to Low Frequency Sound. *Electroanalysis.* 1999;11:401-405. DOI: [https://doi.org/10.1002/\(SICI\)1521-4109\(199905\)11:6<401::AID-ELAN401>3.0.CO;2-6](https://doi.org/10.1002/(SICI)1521-4109(199905)11:6<401::AID-ELAN401>3.0.CO;2-6)
28. Attar T, Harek Y, Larabi L. Determination of Ultra Trace Levels of Copper in Whole Blood by Adsorptive Stripping Voltammetry. *J. Korean Chem. Soc.* 2013;57(5):568-573. DOI: <https://doi.org/10.5012/jkcs.2013.57.5.568>
29. MoutcineA, Chtaini A. Electrochemical determination of trace mercury in water sample using EDTA-CPE modified electrode. *Sens. Bio-Sens. Res.* 2018;17:30-35. DOI: <https://doi.org/10.1016/j.sbsr.2018.01.002>
30. Hassan RYA, Kamel MS, Hassan HNA, Khaled E. Voltammetric determination of mercury in biological samples using crown ether/multiwalled carbon nanotube-based sensor. *J. Electroanal. Chem.*, 2015;759:101-106. DOI: <https://doi.org/10.1016/j.jelechem.2015.10.039>
31. Isaad J, El Achari A. Colorimetric and fluorescent probe based on coumarin for sequential sensing of mercury (II) and cyanide ions in aqueous solutions. *J. Lumin.*, 2022;243:118668. DOI: <https://doi.org/10.1016/j.jlumin.2021.118668>

## DEFINITIONS, ACRONYMS, ABBREVIATIONS

5-Br-PADAP: 2-(5-Bromo-2-pyridylazo)-5-diethylaminophenol

CPE: carbon paste electrode

DPASV: differential pulse anodic stripping voltammetry

EBB R: Eriochrome blue black R

EDTA: Ethylenediamine tetra-acetic acid

EPA: Environmental Protection Agency

GPE: Graphene paste electrode

Hg<sup>2+</sup>: Inorganic mercury

HPLC-ICP-MS: High Performance Liquid Chromatography-inductively coupled plasma-mass spectrometry

LOD: Limit of detection

LOQ: Limit of quantification

MWCNTs: Multiwalled carbon nanotubes

RSD: relative standard deviation

EIS: Electrochemical impedance spectroscopy

UNEP: United Nation Environmental Protection

WHO: World Health Organization